# VICTORIA UNIVERSITY
## MELBOURNE AUSTRALIA

*An effective algorithm for maed problems with a new reliability model at the microgrid*

This is the Published version of the following publication

*Article*

# An Effective Algorithm for MAED Problems with a New Reliability Model at the Microgrid

Amirreza Naderipour [1], Akhtar Kalam [2,*], Zulkurnain Abdul-Malek [1,*], Iraj Faraji Davoudkhani [3], Mohd Wazir Bin Mustafa [4] and Josep M. Guerrero [5]

1    Institute of High Voltage & High Current, School of Electrical Engineering, Faculty of Engineering, Universiti Teknologi Malaysia, Johor Bahru 81310, Malaysia; namirreza@utm.my
2    College of Engineering and Science, Victoria University, Melbourne 3047, Australia
3    Department of Electrical Engineering, Islamic Azad University, Khalkhal Branch, Khalkhal 31367-56817, Iran; faraji.iraj@gmail.com
4    School of Electrical Engineering, Universiti Teknologi Malaysia, Johor Bahru 81310, Malaysia; wazir@utm.my
5    The Villum Center for Research on Microgrids CROM Department of Energy Technology, Aalborg University, 9220 Aalborg East, Denmark; joz@et.aau.dk
*    Correspondence: akhtar.kalam@vu.edu.au (A.K.); zulkurnain@utm.my (Z.A.-M.)

**Abstract:** This paper proposes a new framework for multi-area economic dispatch (MAED) in which the cost associated with the reliability consideration is taken into account together with the common operational and emission costs using expected energy not supplied (EENS) index. To improve the reliability level, the spinning reserve capacity is considered in the model as well. Furthermore, the MAED optimization problem and non-smooth cost functions are taken into account as well as other technical limitations such as tie-line capacity restriction, ramp rate limits, and prohibited operating zones at the microgrid. Considering all the above practical issues increases the complexity in terms of optimization, which, in turn, necessitates the use of a powerful optimization tool. A new successful algorithm inspired by phasor theory in mathematics, called phasor particle swarm optimization (PPSO), is used in this paper to address this problem. In PPSO, the particles' update rules are driven by phase angles to essentially ensure a spread of variants across the population so that exploitation and exploration can be balanced. The optimal results obtained via simulations confirmed the capability of the proposed PPSO algorithm to find suitable optimal solutions for the proposed model.

**Keywords:** microgrid; multi-area economic dispatch (MAED); phasor particle swarm optimization (PPSO); reliability-based MAED; reserve constraints; total pollutant emissions

## 1. Introduction

Thermal generating units constitute a large fraction of electricity production; therefore, the optimal management of such units in the power system is of high importance [1]. Operation of the power system, usually from one hour to one week, mainly belongs to the short-term scheduling problems such as economic load dispatch (ELD) [2] and unit commitment (UC) [3], in which the focus is on the minimization of the operational cost. Accordingly, plenty of research has been carried out addressing ELD using different optimization techniques [4]. On the other hand, an expansion of the ELD optimization issue is the functional multi-area economic dispatch (MAED) optimization problem [5], whose main goal is to evaluate the power generation of generators in various areas and the power exchange between regions [6]. The overall cost of the power grid will reduce. Therefore, following many operating and network constraints [7], taking into account reserve limits in MAED contributes to the problem of reserve constrained multi-area economic dispatch (RCMAED). In addition, the assessment of overall pollutant emissions in RCMAED leads to the reserve restricted multi-area environmental/economic dispatch RCMAEED question [8].

Inclusion of practical considerations (e.g., the valve-point effect, prohibited operating zones, and ramp-rate limitations) in ELD [9] makes the problem sophisticated, which necessitates applying powerful optimization tools to these sorts of problems. Numerous types of methods, including mathematical and meta-heuristic nature-inspired optimization techniques, have been used to tackle the ELD problem in a way to guarantee the optimal solution [10]. Furthermore, authors in [10] solved the RCMAEED problem using the hybridizing sum-local search optimizer (HSLSO) to obtain the optimal solutions. In this respect, economic emission dispatch for thermal units has been pursued by more advanced evolutionary algorithms such as modulated PSO (MPSO) [11] and honey bee mating optimization (HBMO) [12] to utilize the benefits of a faster convergence rate and searching in a wider space. In [13], a novel approach was used based on harmony search (HS) optimization to deal with various types of ED. A new hybrid optimization using Jaya and TLBO has been proposed in [14]. On the other hand, a flower pollination algorithm (FPA) [15], a novel approach using an improved hybrid Jaya algorithm and gradient search method [16], modified stochastic fractal search (SFS) optimization [17], turbulent flow of water-based optimization (TFWO) [18], a new and effective hybrid cuckoo search algorithm (CSA) [19], artificial bee colony optimization (ABCO) [20], large-scale MAED optimization problems integration with wind power [21], chaotic global ABCO [22], and a novel and effective optimizer using Franklin's and Coulomb's laws theory (CFA) [23] have been proposed. For a more comprehensive review, you can refer to [24].

In addition to the common operational cost [25], which is well investigated in generation scheduling studies, the reliability issue is an important factor for power system operators. Interruption in the electricity supplied should be kept at a minimum level to satisfy the costumers' needs [26]. Therefore, the system spinning reserve amount should be sufficient to provide an acceptable level for reliability [27]. To consider this factor, loss of load probability (LOLP) and expected energy not supplied (EENS) are the most effective and prevalent indexes for reliability assessment. As it is obvious, in modern energy management, after considering the common operational cost, it is necessary to consider reliability as well [28].

To cover the various aspects discussed above, this paper presents a new framework for the multi-area economic dispatch, in which the reliability issue together with other technical restrictions are simultaneously taken into account for the first time [29]. To serve this purpose, the EENS index has been added to the formulation and the associated cost is added to the common operational and emission costs. In the model, various constraints such as prohibited operating zones, ramp rate limitations, spinning reserve, and tie-line transmission line capacities are foreseen regarding non-smooth cost functions of thermal units [30]. This paper proposes a powerful modern algorithm called phasor particle swarm optimization (PPSO) to solve various MAED optimization problems, which can be highlighted as the second big contribution of the current study. In mathematics, this algorithm is inspired by the phasor theory and proposes substituting PSO control parameters with variable functions to make PSO a non-parametric algorithm with simpler calculations [31]. The obtained results of this study reveal the effectiveness of the proposed algorithm.

This paper demonstrates that the PPSO algorithm is straightforward and effective for power flow dispatching in electrical systems. All constraints and limitations of the electrical system, in the present study, are assumed with the emission of pollutant gases. Since PSO is a basic algorithm and has been employed in many studies, this version can be used as a base algorithm. There is always a fast convergence problem with the base algorithm in reaching the optimal solution. This issue has been tackled in the proposed version of the algorithm. On the other hand, selecting the best parameters of the algorithm has always been challenging with the base algorithm. The literature shows that different parameters need to be selected for different functions of the basic algorithm. However, the present paper overcomes this issue by presenting and selecting a phase angle, in which all control parameters of the algorithm are assigned to sine and cosine functions of the selected phase angle.

The rest of the paper is organized as follows: first, the formulations of different MAED optimization problems are presented in Section 2. The formulation and flowchart of the proposed PPSO algorithm are presented in Section 3. The simulation results are presented in Section 4, and finally, Section 5 concludes the paper.

## 2. MAED Optimization Problems

### 2.1. Objective Functions

The main objective of various types of MAED in different multi-area power systems is to minimize the total power generation and transmission costs while supplying loads of all the market consumers in all network areas and satisfying electrical transmission capacity constraints, minimum and maximum limits of electrical power generation, and power balance constraints. Minimizing the total pollutant emissions is also one of the objectives that can be considered in MAED. MAED can be expressed in [32]. Given that only real powers (active powers) are considered in solving the economic dispatch problem, power and active power are used interchangeably in this article.

On the other hand, electrical energy generation units are subject to several constraints, including valve-point loading on the objective function of the problem. This constraint causes the objective function to lose its flatness and convert into a sine objective function. There are always several types of fuels with different prices in an energy generation system for feeding electrical energy generation units. Thus, the objective function is transformed into a multi-type objective function. This paper applied these two constraints together to the problem.

#### 2.1.1. Minimizing Operational Cost Considering Reliability Issues

The objective function of the single area economic dispatch problem can be expressed as [33]

$$Min \sum_{n=1}^{N} (F_n(P_n)) \tag{1}$$

where

1: $$F_n(P_n) = \begin{cases} a_{n1}P_n^2 + b_{n1}P_n + c_{n1} + |e_{n1} \times \sin(f_{n1} \times (P_{n,\min} - P_n))|, & fuel 1, \quad P_{n,\min} \le P_n \le P_{n1} \\ \dots \\ a_{nk}P_n^2 + b_{nk}P_n + c_{nk} + |e_{nk} \times \sin(f_{nk} \times (P_{n,\min} - P_n))|, & fuel\ k, \quad P_{nk-1} \le P_n \le P_{nk} \\ \dots \\ a_{nk}P_n^2 + b_{nk}P_n + c_{nk} + |e_{nk} \times \sin(f_{nk} \times (P_{n,\min} - P_n))|, & fuel\ k, \quad P_{nk-1} \le P_n \le P_{n,\max} \end{cases}$$

2: $n$ is the index of available generation units and $N$ is the number of available generation units.

3: $k$ is the index fuel type and $K$ is the number of fuel types.

4: $P_n$ is the output power of the $n$th unit and $P_{n,\max}$ and $P_{n,\min}$ are maximum and minimum output power limits of the $n$th unit, respectively.

5: $a_{nk}P_n^2 + b_{nk}P_n + C_{nk}$ is a quadratic generation cost function for fuel type $k$ of the $n$th unit.

6: $a_{nk}$, $b_{nk}$, and $c_{nk}$ are cost function coefficients of the $n$th unit for fuel type $k$.

7: $|e_{nk} \times \sin(f_{nk} \times (P_{n,\min} - P_n))|$ is sinusoidal and the non-smooth fuel cost function due to the VPL effects for fuel type $k$ of the $n^{th}$ unit.

8: $e_{nk}$ and $f_{nk}$ are cost function coefficients of the VPL effects model of the $n$th unit for fuel type $k$.

The cost function of MAED must consider the cost of power transmission through transmission lines. Thus, Equation (1) would change as [34]:

$$MinF_T = Min(\sum_{n=1}^{N} (F_n(P_n)) + \sum_{j=1}^{M} (f_j(T_j))) \tag{2}$$

where $M$ is the number of transmission lines, $f_j$ is the cost function associated with the $j$th line, and $T_j$ is the active power flow through the $j$th line.

As previously mentioned, consideration of reliability in the MAED is the main goal of this paper. In most cases, loss of load probability (LOLP) and expected energy not supplied (EENS) indices are taken into account, as the most well-known reliability indices, for reliability assessment. Indeed, the former models the failure probability of the system [28], while the latter implies the concept of basic energy not supplied. This paper includes the EENS index in the objective function. Therefore, the objective function (2) can be updated as (3). In addition, EENS is formulated through Equations (4)–(9) [20].

$$Min \; F_T = Min \left( \sum_{n=1}^{N} (F_n(P_n)) \; + \; \sum_{j}^{M} (f_j(T_j)) \; + \; EENS \times c_{ens} \right) \tag{3}$$

$$EENS = \sum_{lp=1}^{LP} \left( EPNS_{lp} \times TD_{lp} \right) \tag{4}$$

$$EPNS_{lp} = \begin{cases} Probability_{lp} \times \left( P_{lp}^L - P_{lp}^G \right) & P_{lp}^L > P_{lp}^G \\ 0 & P_{lp}^L \leq P_{lp}^G \end{cases} \tag{5}$$

$$Probability_i = \left( \prod_{H' \in X} U_{H'} \right) \times \left( \prod_{H \in Y} (1 - U_H) \right) \tag{6}$$

$$U_n = \frac{FR_n}{FR_n + RR_n} = \frac{MTTR_n}{MTTF_n + MTTR_n} \tag{7}$$

$$T_{Failure,n} = \frac{1}{FR_n} \tag{8}$$

$$T_{Repair,n} = \frac{1}{RR_n} \tag{9}$$

According to Equation (4), EENS is the summation of all the load points of EPNS indices multiplied by their durations ($TD_{lp}$), which shows the total value of EENS. In addition, $TD_{lp}$ can be obtained from Figure 1. As can be observed, it is simple to obtain the period of two defined load points with their related data as the number of hours that energy usage is equivalent to a certain load level. Furthermore, based on Equation (5), $EPNS_{lp}$ indicates the value of power not supplied at the $lp^{th}$ load point, where $P_{lp}^L$ is the value of load demand at the $lp^{th}$ load point and $P_{lp}^G$ is the total output powers of available generation units at the $lp^{th}$ load point. The $EPNS_{lp}$ value depends on the unavailability of generators, that is $Probability_{lp}$, which is defined by Equation (6), where $X/Y$ is the set of available (unavailable) generation units at the $lp^{th}$ load point. The mentioned probability expresses the concept of generators failure rate and mean time to repair, which are formulated using Equations (8) and (9), respectively.
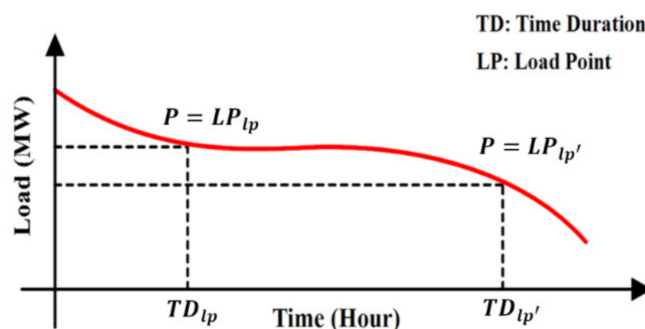


**Figure 1.** The diagram of load duration.

### 2.1.2. Minimizing Emissions

One of the issues with electrical energy generation units is the use of fossil fuels. Several types of gases are emitted into the environment when fossil fuels are burnt, hence leading to pollution and destruction of nature. To overcome this problem, designers and engineers consider the emission level of these generation units as an objective function that depends on the generation power of the units during the design and optimization phases. This is formulated as follows [9]:

$$Min \, F_T = Min \sum_{n=1}^{N} E_n(P_n) \tag{10}$$

where

1: $E_n(P_n) = \begin{cases} a_{n1}P_n^2 + \beta_{n1}P_n + \gamma_{n1}, & fuel1, \quad P_{n,\min} \leq P_n \leq P_{n1} \\ \dots \\ a_{nk}P_n^2 + \beta_{n1}P_n + \gamma_{n1}, & fuel \, k, \quad P_{nk-1} \leq P_n \leq P_{nk} \\ \dots \\ a_{nk}P_n^2 + \beta_{nk}P_n + \gamma_{nk}, & fuel \, k, \quad P_{nk-1} \leq P_n \leq P_{n,\max} \end{cases}$

2: $a_{nk}P_n^2 + \beta_{nk}P_n + \gamma_{nk}$ is emission generated by the $n$th unit for fuel type $k$.

3: $a_{nk}, \beta_{nk}$, and $\gamma_{nk}$ are the emission coefficients of the $n$th unit for fuel type $k$.

### 2.2. Constraints

In an energy generation system, designers and engineers always encounter several constraints that need to be satisfied. These constraints depend on the units, transmission lines, system demand level, and the system total loss level. Each of these constraints is provided and formulated.

### 2.2.1. Area Total Active Power Balance

The total active power balance constraint of area q of the network neglecting the electrical system power losses can be given as [8]

$$\sum_{n=1}^{N_q} (P_n) = \left( P_{Loadq} + \sum_{w \in M_q} T_{qw} \right) \tag{11}$$

where $N_q$ is the number of committed generating units for the $q$th area, $P_{Loadq}$ is the power demand in the $q$th area, and $M_q$ is the set of all areas connected to the $q$th area via a tie-line.

### 2.2.2. Generator Output Power Limits

The generating capacity of the generator units is constrained to their minimum and maximum limits, as follows [9]:

$$P_{n,\min} \leq P_n \leq P_{n,\max} \,, \quad i = 1, \dots, N \tag{12}$$

### 2.2.3. Ramp-Rate Limits

This constraint can be formulated as expressed in (13) [35]:

$$\max(P_{n,\min,} \leq P_n^0 - DR_n \leq P_n \leq \min(P_{n,\max,} \leq P_n^0 + UR_n)) \tag{13}$$

where $p_n^0$ is the power output of the $n$th generation unit in the previous stage, and the $DR_n$ and $Un_i$ are ramp-up and ramp-down rate limits of the $n$th thermal generator, respectively. This constraint determines the lower and upper bounds of the objective variables.

### 2.2.4. Prohibited Operating Zones (POZ) Due to Physical Operational Limitations

In thermal generating units, the input-output power generation curve with the POZ specifications can be formulated as presented in the following equation [9]:

$$P_n \in \begin{cases} P_{n,\min} \leq P_n \leq P_{n1}^1 \\ \dots \\ P_{nh-1}^u \leq P_n \leq P_{nh}^1 \\ \dots \\ P_{nzn}^u \leq P_n \leq P_n^{\max} \end{cases} \tag{14}$$

where $h$ is the index of POZs of the $n$th unit, $zn$ is the number of POZ in input-output power curve of the $n$th thermal generating unit, $P_{ih}^1$ and $P_{ih}^u$ are the minimum and maximum limits of the $h$th POZ of the $n$th thermal unit, respectively. In optimization, the optimization variables located in a POZ are set to the lower or upper limit of the POZ, the one closer to their values.

### 2.2.5. Maximum and Minimum Power Transfer Through Tie-Lines

The tie-line power flow from the $q$th area to the $w$th area ($T_{qw}$) must not violate the maximum tie-line power transfer capacity limit ($T_{qw,\max}$) [8].

$$\left| T_{qw} \right| \leq T_{qw,\max}, \quad w \in M_q \tag{15}$$

### 2.2.6. Spinning Reserve (SR) Requirement in Each Area

In each area, a spinning reserve should be set to encounter the support system adequacy and stability in the case of contingency. Better fulfilment of the necessary SR can be achieved by multi-area reserve sharing [36]. The reserve constraint can be formulated for the $q$th area as [9]:

$$\sum_{n=1}^{N_q} S_n + \sum_{w \in M_q} RC_w \geq S_{q,req} \tag{16}$$

where $\sum_{n=1}^{N_q} S_n$ is the reserve provided by all the generation units of the $q$th area, which can be considered as $\sum_{n=1}^{N_q} P_n^{\max} - P_n$, $S_{q,req}$ is the SR requirement in the $q$th area, and $\sum_{w \in M_q} RC_w$ is the sum of reserves contributed from other areas to the $q$th area.

### 2.2.7. Limitation on Power Transfers Considering SR Contribution

The minimum and maximum active power transfer limits through tie-lines must be revised to account for the reserve contribution ($RC_{qw}$), as follows [36]:

$$\max\{\left| T_{qw} \right|, \left| T_{qw} + RC_{qw} \right|\} \leq T_{qw,\max}, \quad w \in M_q \tag{17}$$

Therefore, the original objective function of a practical MAEED problem can be amplified by the following equation [9]:

$$\mathrm{Min}F_T = \mathrm{Min} \left( \begin{array}{c} \sum\limits_{n=1}^{N} (F_n(P_n)) + \sum\limits_{j=1}^{M} (f_j(T_j)) + \phi \times \sum\limits_{n=1}^{N} (En(P_n)) + \dots \\ \lambda \times \left| \sum\limits_{N=1}^{N} (P_n) - P_{Load} \right| + \lambda \times (g_1 + g_2) \end{array} \right) \tag{18}$$

where $\phi$ is a suitable value selected by the user (in this study: 120), $\lambda$ is an appropriate penalty coefficient value, and $P_{Load}$ is the entire real load demand in the system. $g_1$ is $\max(|T_{qw}| - T_{qw,\max}, 0)$ in MAED problem and $\max(\max\{|T_{qw}| - T_{qw} + RC_{qw}\} - T_{qw,\max}, 0)$ in RCMAED and RCMAEED problems. $g_2$ is 0 for the MAED problem and

$$\sum_{q=1}^{NA} \max(S_{q,req} - \sum_{n=1}^{N_q} S_{nq} - \sum_{w \in M_q} RC_{wq}, 0), \; w \in M_q \text{ for the RCMAED and RCMAEED prob-}$$

lems (NA denotes the number of areas).

## 3. Phasor Particle Swarm Optimization (PPSO) Technique

This section introduces the original PSO algorithm as well as a number of its common and popular versions. Then, the method proposed and employed in this study, called phasor particle swarm optimization (PPSO), is described.

### 3.1. Background of Different Variants of PSO

In [37], a review of novel PSO-based algorithms can be found. Each swarm particle in the basic PSO has a current position vector and a current velocity vector. The current position vector of the *i*th particle, for instance, is [23]

$$X_i = [x_{i1}, x_{i2}, \dots, x_{iD}] \tag{19}$$

and its current velocity vector is [23]

$$V_i = [v_{i1}, v_{i2}, \dots, v_{iD}] \tag{20}$$

At the start of the optimization process, these vectors are started arbitrarily. With the use of its current position and velocity vectors, the position and velocity of the *i*th particle are updated. In this system, the best position the *i*th particle has experienced so far is the best personal position vector, *Pbest$_i$*, and the best position all particles have experienced so far is the best global position vector, *Gbest*.

The optimization phase is carried out in each iteration of the algorithm based on design knowledge to maximize the objective function (f). In each new iteration, therefore, a new velocity ($V_i^{Iter+1}$) is generated, using the following equation for d = 1, 2, ... D [24]:

$$v_{id}^{Iter+1} = v_{id}^{Iter} + c_1 \times r_{id}^1 \times (pbest_{id}^{Iter} - x_{id}^{Iter}) + c_2 \times (gbest_{id}^{Iter} - x_{id}^{Iter}) \tag{21}$$

where $c_1$ and $c_2$ are acceleration control coefficients, which can be chosen by the designer, $r1_{id}$ and $r2_{id}$ are uniform random coefficients in the range of (0, 1), and Iter is the number of the current iteration.

Particle velocity values, $V_i$, are constrained to the range defined to prevent particles [8] from travelling out of the issue search room.

Each particle's location is then modified as follows [24]:

$$X_i^{Iter+1} = X_i^{Iter} + V_i^{Iter+1} \tag{22}$$

Using the following equation, the personal best position is updated for each particle [23]:

$$Pbest_i^{Iter+1} = \begin{cases} Pbest_i^{Iter}, if \; f(Pbest_i^{Iter}) \leq f(X_i^{Iter+1}) \\ X_i^{Iter+1}, \; otherwise \end{cases} \tag{23}$$

Using the following equation, the best global population position is updated [23]:

$$Gbest_i^{Iter+1} == \begin{cases} Pbest_i^{Iter}, if > f(Pbest_i^{Iter+1}) \leq f(Gbest^{Iter}) \\ X_i^{Iter}, \; otherwise \end{cases} \tag{24}$$

A modified PSO algorithm (PSO-ω) was introduced by Shi and Eberhartin [24], in which the inertia weight was presented to balance the local and global search. In PSO-ω, each particle's new velocity is calculated as follows [23]:

$$v_{id}^{Iter+1} = \omega^{iter} \times v_{id}^{Iter} + c_1 \times r_{id}^1 \times (Pbest_i^{Iter} - x_{id}^{Iter}) + c_2 \times r_{id}^2 \times (gbest_i^{Iter} - x_i^{Iter}) \tag{25}$$

In [24], the proposed $\omega$ is linearly decreased from $\omega_{\max}(=\omega^{iter=1})$ (initial value) to $\omega_{\min}(=\omega^{iter\ \max})$ (final value) during the optimization process as follows [23]:

$$\omega^{Iter} = \omega_{\max} - (\omega_{\max} - \omega_{\min}) \times \frac{Iter}{Iter_{\max}} \tag{26}$$

The paper proposed 0.9 and 0.4 for $\omega_{\max}$ and $\omega_{\min}$ values, respectively.

An updated PSO algorithm was proposed by Clerc and Kennedy [38] using a new control parameter, called the constriction factor $\chi$, which improves the PSO convergence speed by changing Equation (25) to the one below [38]:

$$v_{id}^{Iter+1} = \chi(v_{id}^{Iter} = +c_1 \times r_{id}^1 \times (Pbest_{id}^{Iter} - x_{id}^{Iter}) + c_2 \times r_{id}^2 \times (gbest_{id}^{Iter} - x_{id}^{Iter})) \tag{27}$$

It is centered on the control coefficient values $c_1 = c_2 = 2.05$, where the control parameter $\chi$ is set to 0.729 using Equation (28) [38]:

$$\chi = \frac{2}{\left| 2 - (c_1 + c_2) - \sqrt{(c_1 + c_2)^2 - 4(c_1 + c_2)} \right|} \tag{28}$$

In the current paper, a new version of PSO, called phasor particle swarm optimization (PPSO), is suggested, which is motivated by the phasor theory in mathematics. In the suggested PPSO process, all control variables are put in the algorithm-generated step angle $\theta$. This renders the PSO (which has simplified equations) a non-parametric algorithm. In contrast with other algorithms, the best benefits of the proposed PPSO algorithm are the improvement in optimization performance considering the increase in the problem dimension. To solve real-parameter problems, the proposed algorithm, which is defined in the following pages, can be effectively used.

*3.2. Parameter Setting in PPSO*

In this paper, two periodic trigonometric functions, i.e., cos$\theta$ and sin$\theta$, and their absolute values are used to create PSO control parameters. cos$\theta$ and sin$\theta$ are periodic functions with a period of 0 to $2\pi$ radians (6.2832) and have values in the range of $-1$ to 1. Periodic functions with periods of $\pi$ radians and values in the range of 0 and 1 are also their absolute values.

The periodic nature of these functions is used to substitute the phase angle $\theta$ for all control parameters of the PSO algorithm and to transform them into $\theta$ functions to accomplish various strategies. For this reason, a one-dimensional phase angle, $\theta_i$, is defined for each particle so that, for example, the *i*th particle could be modelled by a magnitude vector $\overrightarrow{X_i}$ with angle $\theta_i$ and represented as $\overrightarrow{X_i}\angle\theta$.

The periodic nature of these functions is used to replace all control parameters of the PSO algorithm by phase angle $\theta$ and to convert them to functions $\theta$ to reach different strategies. For this purpose, a one-dimensional phase angle, $\theta_i$, is defined for each particle such that, for example, the *i*th particle could be modeled by a magnitude vector $\overrightarrow{X_i}$ with angle $\theta_i$ and represented as $\overrightarrow{X_i}\angle\theta$.

The value of $\omega$ is set to zero ($\omega = 0$) for the proposed PPSO algorithm, the same as for PSO-TVAC in [39] and even the current model; this approach can, however, be established for other improved PSO algorithms. The suggested particle motion model is as follows [40]:

$$v_i^{Iter} = p(\theta_i^{Iter}) \times (Pbest_i^{Iter} - X_i^{Iter}) + g(\theta_i^{Iter}) \times (Gbest^{Iter} - X_i^{Iter}) \tag{29}$$

By testing different $p(\theta_i^{Iter})$ and $g(\theta_i^{Iter})$ functions for PPSO on real test functions, the following functions were selected.

The following functions were chosen by evaluating various $p(\theta_i^{Iter})$ and $g(\theta_i^{Iter})$ functions for PPSO on actual test functions [40]:

$$p(\theta_i^{Iter}) = \left|\cos\theta_i^{Iter}\right|^{2*\sin\theta_i^{Iter}} \tag{30}$$

$$g(\theta_i^{Iter}) = \left|\sin\theta_i^{Iter}\right|^{2*\cos\theta_i^{Iter}} \tag{31}$$

It is possible to obtain all the appropriate behaviours and techniques using these $p(\theta_i^{Iter})$ and $g(\theta_i^{Iter})$ functions throughout the running of the algorithm. Often, all of these tasks together raise or decrease and their actions are sometimes inverse.

There is also the probability, in a particular step angle, that these functions become identical to each other. Therefore, it is conceivable that a broad value is achieved by one of the functions. Such behaviours generate adaptive search functions, which are originally produced by control parameters, utilizing only particle-phase angles. This provides a balance between global search and local search, and an adaptive and non-parametric algorithm is converted by the algorithm. These quick or sluggish increases or decreases in the same or opposite direction(s) of $p(\theta_i^{Iter})$ and $g(\theta_i^{Iter})$ enable the algorithm to escape from premature convergence to an ideal local solution.

### 3.3. Flowchart of PPSO

Figure 2 shows the flowchart of the PPSO algorithm, which is close to other PSO algorithms. First, $N_{Pop}$ random particles (initial population) $\vec{X_i} = |X_i| < \theta_i$ ($i$ = 1: $N_{Pop}$) are generated in the D-dimensional space of the problem with their phasor angle $\theta_i$ with uniform distribution $\theta_i^{Iter=1} = U(0, 2\pi)$ and with the initial speed limit $v_{max,i}^{Iter=1}$. Then, the velocity of each particle in each iteration of the algorithm is updated with the following equation [40]:

$$v_i^{Iter} = \left|\cos\theta_i^{Iter}\right|^{2*\sin\theta_i^{Iter}} \times (Pbest_i^{Iter} - X_i^{Iter}) + \left|\sin\theta_i^{Iter}\right|^{2*\cos\theta_i^{Iter}} \times (Gbest^{Iter} - X_i^{Iter}) \tag{32}$$

Then, the new position of the particle is updated using the equation presented below:

$$\vec{X_i}^{Iter+1} = \vec{X_i}^{Iter} + \vec{V_i}^{Iter} \tag{33}$$

Next, $P_{best}$ and $G_{best}$ are determined, similar to the original PSO algorithm.

The step angle and overall particle velocity are then modified using the following equations for the next iteration [40]:

$$\theta_i^{Ite+1} = \theta_i^{Iter} + T(\theta) \times (2\pi) = \theta_i^{Iter} + \left|\cos\theta_i^{Iter}\right| + \left|\sin\theta_i^{Iter}\right| \times (2\pi) \tag{34}$$

$$V_{i,max}^{Iter+1} = W(\theta) \times (X_{max} - X_{min}) = \left|\cos\theta_i^{Iter}\right|^2 \times (X_{max} - X_{min}) \tag{35}$$
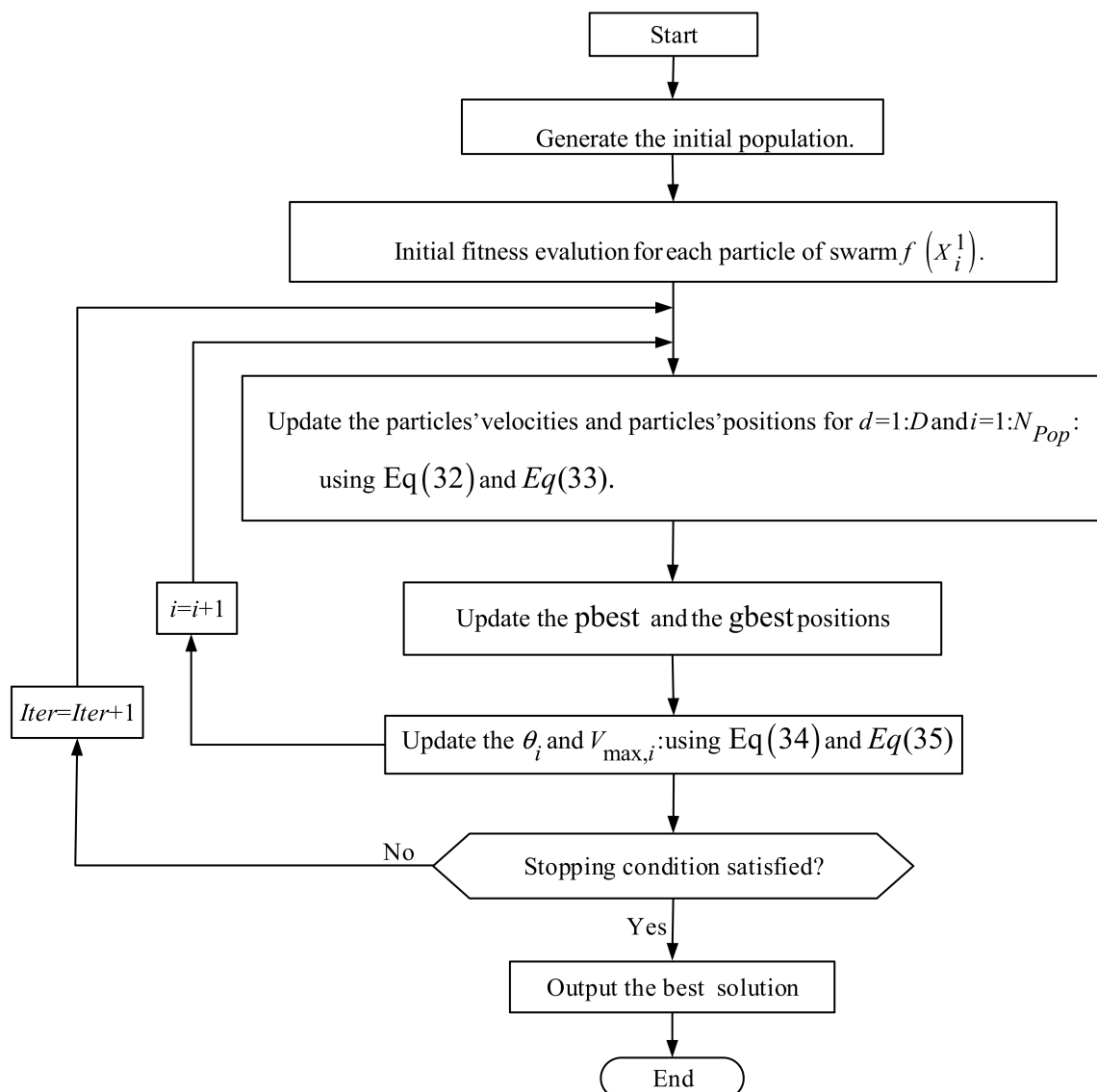
**Figure 2.** Flowchart of the proposed phasor particle swarm optimization (PPSO) algorithm process.

### 4. Results and Discussion

*4.1. Optimization Results*

The proposed PPSO algorithm was evaluated on three case studies of practical MAED problems in three different multi-area power systems: (1) a two-area test power system comprising four electrical power generators as a small-scale test MAED optimization problem, (2) a four-area test power system comprising 16 electrical power generators for MAED, RCMAED, and RCMAEED optimization problems, and (3) a two-area test power system comprising 40 electrical power generators as a large-scale test MAED problem. The results of PPSO were compared with those of previously-improved variants of PSO in the literature such as adaptive PSO (APSO) [41], comprehensive learning PSO (CLPSO) [42], the improved standard PSO 2011 (SPSO2011) [43], fully informed particle swarm (FIPS) [44], and Frankenstein's PSO (FPSO) [45].

4.1.1. The MAED Problems Optimization Process Using PPSO

The steps involved in the algorithm of the proposed PPSO optimizer for solving MAED problems with non-smooth objective functions in multi-area power systems are as follows:

**Step 1:** Setting the control parameters and the required data of the power system and generation units in the multi-area network.

**Step 2:** Producing the initial random phasor particle swarm of the PPSO optimizer as follows [9]:

$$P_n^L = \max\left\{P_{n,\min}, P_n^0 - DR_n\right\}, P_n^U = \min\left\{P_{n,\max}, P_n^0 - UR_n\right\}, \\ P_n^L \leq P_n \leq P_n^U \tag{36}$$

$$\left[X_{j,i}^0\right]_{D \times N_{pop}} = \left[P_n^L + rand_{j,n}(0,1) \times (P_n^U - P_n^L)\right]_{D \times N_{pop}} \tag{37}$$

**Step 3:** Calculating the objective function values of the MAED problem, while imposing constraints of the generation units and multi-area network.

**Step 4:** Producing a new particle phasor swarm of the PPSO optimizer using Equation (32) to (35).

**Step 5:** Calculating the objective of the MAED problem.

**Step 6:** Repeating steps 4 and 5 until the iterations are finished.

### 4.1.2. Practical MAED Optimization Problems

(a) The small-scale test system

The under-study system uses fossil fuel; thus, we need to consider the emission levels of units. The small-scale test system is a two-area power system comprising four electrical power generators whose data were extracted from [12,32–34], and its tie-line power flow limit and total power demand are 200 MW and 1120 MW, respectively. The demand in area 1 (comprising units 1 and 2) is 70% of the total demand, and the demand in system area 2 (comprising units 3 and 4) is 30% of the total demand [8]. The best global optimal solution of this test system was obtained using each of the PSO algorithms in 30 separate runs with a maximum number of iterations equal to 100 and maximum population size equal to $N_{Pop} = 80$. This table represents the results of PPSO, APSO, CLPSO, SPSO2011, FPSO, FIPS, PSO-TVAC [8], Hopfield neural network (HNN) method [46], and direct search method (DSM) [47]. Table 1 shows that the minimum operation and fuel cost obtained by the PPSO optimizer was 10,604.6741 ($/H), which was less than that of HNN [46], DSM [47], and PSO-TVAC [8].

**Table 1.** Comparison of the best solutions obtained for the small-scale test system.

| Method | $P_1$ (MW) | $P_2$ (MW) | $P_3$ (MW) | $P_4$ (MW) | $T_{12}$ (MW) | $\sum P_g$ | Cost ($/H) |
|---|---|---|---|---|---|---|---|
| HNN [46] | - | - | - | - | - | - | 10,605 |
| DSM [47] | - | - | - | - | - | - | 10,605 |
| PSO-TVAC [8] | 444.8047 | 139.1953 | 211.0609 | 324.9391 | −200 | 1120 | 10,604.68 |
| PPSO | 445.1223 | 138.8778 | 212.0426 | 323.9573 | −199.9999 | 1120 | 10,604.67 |
| APSO | 445.3207 | 138.6794 | 212.2054 | 323.7945 | −199.9999 | 1120 | 10,604.67 |
| CLPSO | 445.1213 | 138.8788 | 212.0413 | 323.9586 | −199.9999 | 1120 | 10,604.67 |
| SPSO2011 | 445.1223 | 138.8778 | 212.0426 | 323.9573 | −199.9999 | 1120 | 10,604.67 |
| FPSO | 445.0654 | 138.9347 | 211.9258 | 324.0741 | −199.9999 | 1120 | 10,604.67 |
| FIPS | 445.2274 | 138.7727 | 211.9977 | 324.0022 | −199.9999 | 1120 | 10,604.67 |

(b) The medium-scale test system

This medium-scale system is a four-area power system comprising 16 electrical power generators, whose data, including data of power generating units and tie-line minimum and maximum flow limits, were extracted from [48–50]. The power demands are 400 MW in area 1 (comprising units 1 to 4), 200 MW in area 2 (comprising units 5 to 8), 350 MW in area 3 (comprising units 9 to 12), and 300 MW in area 4 (comprising units 13 to 16). The maximum number of iterations and the maximum population size of all PSO algorithms are set to 250 and $N_{Pop} = 80$, respectively. The best global optimal solution obtained by the proposed PPSO optimizer and the best global optimal solutions reported in the literature for the medium-scale test system are presented in Table 2. The global optimal solution to which the proposed PPSO optimizer reached is feasible ($\sum P_g = 1250.0$ MW),

but the best results reported in previous studies using other algorithms, e.g., PSO algorithms, the classical evolutionary programming (CEP) method [51], the hybrid harmony search (HHS) algorithm [48], the network flow programming (NFP) method [52], and the pattern search (PS) algorithm [53] are not feasible. Additionally, the solution obtained by the PPSO optimizer is better than that of the hybridizing sum-local search optimizer (HSLSO) [10] algorithm.

**Table 2.** The best solutions obtained for the medium-scale test system.

| Area No. | | PSO [10] | HHS [48] | NFP [52] | CEP [51] | PS [53] | HSLSO [10] | PPSO |
|---|---|---|---|---|---|---|---|---|
| 1 (400 MW) | $P_1$ (MW) | 150 | 150 | 150 | 150 | 150 | 150 | 150 |
| | $P_2$ (MW) | 100 | 100 | 100 | 100 | 100 | 100 | 100 |
| | $P_3$ (MW) | 67.366 | 66.86 | 66.97 | 68.826 | 66.971 | 67.3848 | 67.31016 |
| | $P_4$ (MW) | 100 | 100 | 100 | 99.985 | 100 | 100 | 100 |
| 2 (200 MW) | $P_5$ (MW) | 56.613 | 57.04 | 56.97 | 56.373 | 56.9718 | 57.0625 | 57.07953 |
| | $P_6$ (MW) | 95.474 | 96.22 | 96.25 | 93.519 | 96.2518 | 96.1749 | 96.34877 |
| | $P_7$ (MW) | 41.617 | 41.74 | 41.87 | 42.546 | 41.8718 | 41.8472 | 41.86785 |
| | $P_8$ (MW) | 72.356 | 72.5 | 72.52 | 72.647 | 72.5218 | 72.4505 | 72.53403 |
| 3 (350 MW) | $P_9$ (MW) | 50 | 50 | 50 | 50 | 50.002 | 50 | 50 |
| | $P_{10}$ (MW) | 35.973 | 36.24 | 36.27 | 36.399 | 36.272 | 36.319 | 36.28298 |
| | $P_{11}$ (MW) | 38.21 | 38.39 | 38.49 | 38.323 | 38.492 | 38.5911 | 38.50812 |
| | $P_{12}$ (MW) | 37.162 | 37.2 | 37.32 | 36.903 | 37.322 | 37.3719 | 37.26609 |
| 4 (300 MW) | $P_{13}$ (MW) | 150 | 150 | 150 | 150 | 150 | 150 | 150 |
| | $P_{14}$ (MW) | 100 | 100 | 100 | 100 | 100 | 100 | 100 |
| | $P_{15}$ (MW) | 57.83 | 56.9 | 57.05 | 56.648 | 57.051 | 56.9272 | 56.9218 |
| | $P_{16}$ (MW) | 97.349 | 96.2 | 96.27 | 95.826 | 96.271 | 95.8709 | 95.88068 |
| Tie-line power flow | $T_{12}$ (MW) | 0 | 0 | 0 | −0.018 | 0 | 0 | 0 |
| | $T_{13}$ (MW) | 22.588 | 16.86 | 18.18 | 19.587 | 18.181 | 17.4643 | 17.42629 |
| | $T_{14}$ (MW) | −5.176 | 0 | −1.21 | −0.758 | −1.21 | −0.0795 | −0.116132 |
| | $T_{23}$ (MW) | 66.064 | 70.61 | 69.73 | 68.861 | 69.73 | 70.2537 | 70.51652 |
| | $T_{24}$ (MW) | −0.004 | −3.11 | −2.11 | −1.789 | −2.111 | −2.7186 | −2.686341 |
| | $T_{34}$ (MW) | −100 | −100 | −100 | −99.927 | −100 | −100 | −100 |
| $\sum P_g$ (MW) | | 1249.95 | 1249.29 | 1249.98 | 1247.995 | 1249.998 | 1250 | 1250 |
| Cost ($/H) | | 7336.93 | 7329.85 | 7337 | 7337.75 | 7336.98 | 7337.03 | 7337.026 |

(c)　The large-scale test system

The large-scale test system is a two-area power system that has 40 electrical power generators with ramp rate limits, VPL effects, and POZ [8]. The generating units 1 to 20 are in area 1 and generating units 21 to 40 are in area 2. The total power demand is 10,500 MW, from which 7500 MW is the power demand in area 1 and 3000 MW is the power demand in system area 2. The maximum power transfer between the two areas is 1500 MW. Table 3 compares the best global optimal solution obtained using the proposed PPSO optimizer with that of a chaotic differential evolution algorithm (DEC2) [8] and the HSLSO algorithm [10] with a maximum number of iterations equal to 500 and maximum population size equal to $N_{Pop} = 80$. Table 3 shows that the new PPSO optimizer can converge to a better-quality solution in solving a large-scale MAED problem with different practical constraints, whose cost is 125,100.2436 ($/H).

The best, mean, and Std (standard deviation) indexes of the best objective function values for 30 trials of all PSO algorithms for different multi-area power systems are shown in Table 4. Referring to this table and Figure 3, the proposed algorithm has the best standard deviation for the best-obtained solutions. Consequently, it can be claimed that the suggested method is the most reliable method among the methods studied to optimize such problems and also confirms that the PPSO optimizer performance was better than all other algorithms in terms of achieving the optimal solutions of the small-scale MAED optimization problem. It can be seen that the PPSO optimizer provides better quality and more suitable optimal results among all the PSO algorithms.

**Table 3.** Best solutions obtained for the large-scale test system.

| Area 1 (PD = 7500 MW) | | | | Area 2 (PD = 3000 MW) | | | |
|---|---|---|---|---|---|---|---|
| Output (MW) | DEC2 [8] | HSLSO [10] | PPSO | Output (MW) | DEC2 [8] | HSLSO [10] | PPSO |
| $P_1$ | 112.8292 | 110.8012 | 110.8012 | $P_{21}$ (MW) | 343.7598 | 523.2792 | 523.2794 |
| $P_2$ | 114 | 113.9997 | 113.9998 | $P_{22}$ (MW) | 433.5196 | 523.2791 | 523.2794 |
| $P_3$ | 97.3999 | 120 | 120 | $P_{23}$ (MW) | 523.2794 | 523.2794 | 523.2795 |
| $P_4$ | 179.7331 | 179.7331 | 179.7332 | $P_{24}$ (MW) | 550 | 523.2794 | 523.2794 |
| $P_5$ | 97 | 95.551 | 95.5504 | $P_{25}$ (MW) | 550 | 523.2795 | 523.2793 |
| $P_6$ | 68.0001 | 140 | 140 | $P_{26}$ (MW) | 254 | 254 | 254 |
| $P_7$ | 300 | 300 | 300 | $P_{27}$ (MW) | 10 | 10.0001 | 10 |
| $P_8$ | 284.5997 | 284.5997 | 284.5997 | $P_{28}$ (MW) | 10.0001 | 10 | 10 |
| $P_9$ | 284.5997 | 284.5997 | 284.5997 | $P_{29}$ (MW) | 10 | 10 | 10 |
| $P_{10}$ | 130 | 270 | 270 | $P_{30}$ (MW) | 47 | 87.7997 | 87.7997 |
| $P_{11}$ | 360 | 94 | 94.0002 | $P_{31}$ (MW) | 159.7331 | 188.5959 | 188.5954 |
| $P_{12}$ | 94.0001 | 300 | 300 | $P_{32}$ (MW) | 190 | 159.7331 | 159.7331 |
| $P_{13}$ | 304.5196 | 304.5195 | 304.5195 | $P_{33}$ (MW) | 163.7269 | 159.733 | 159.7331 |
| $P_{14}$ | 500 | 394.2797 | 394.2793 | $P_{34}$ (MW) | 164.7998 | 164.8002 | 164.8 |
| $P_{15}$ | 484.0392 | 484.0395 | 484.0395 | $P_{35}$ (MW) | 200 | 164.7998 | 164.7998 |
| $P_{16}$ | 500 | 484.0391 | 484.0391 | $P_{36}$ (MW) | 164.7998 | 164.7998 | 164.7992 |
| $P_{17}$ | 489.2794 | 489.2794 | 489.2797 | $P_{37}$ (MW) | 110 | 89.1143 | 89.1143 |
| $P_{18}$ | 500 | 489.2796 | 489.2794 | $P_{38}$ (MW) | 57.0571 | 89.114 | 89.1142 |
| $P_{19}$ | 550 | 549.9998 | 549.9998 | $P_{39}$ (MW) | 25 | 89.1134 | 89.1142 |
| $P_{20}$ | 550 | 511.2791 | 511.2794 | $P_{40}$ (MW) | 511.2794 | 242.0001 | 242 |
| $T_{12}$ (MW) | −1500 | −1500 | −1500 | Cost ($/H) | 127,344.9 | 125,100.3 | 125,100.2 |

**Table 4.** Comparing the simulation final results for the multi-area power systems.

| Test System | Index | FIPS | FPSO | SPSO2011 | CLPSO | APSO | PPSO |
|---|---|---|---|---|---|---|---|
| small-scale system | Best | 10,604.6742 | 10,604.67 | 10,604.6741 | 10,604.67 | 10,604.67 | 10,604.67 |
| | Mean | 10,605.3272 | 10,604.92 | 10,604.8543 | 10,604.68 | 10,604.73 | 10,604.67 |
| | Std | 1.5275 | 1.1547 | 0.5774 | 0.7022 | 0.4407 | $5.75 \times 10^{-5}$ |
| | Mean time (s) | 4.56 | 4.78 | 4 | 3.16 | 6.82 | 2.93 |
| medium-scale system | Best | 7341.7942 | 7340.455 | 7340.2795 | 7344.357 | 7341.714 | 7337.026 |
| | Mean | 7559.7788 | 7487.087 | 7637.4443 | 7486.892 | 7605.919 | 7338.115 |
| | Std | 74.2674 | 61.8126 | 71.271 | 84.3494 | 53.07 | 0.629 |
| | Mean time (s) | 20.95 | 20.67 | 19.19 | 18.31 | 25.57 | 17.84 |
| large-scale system | Best | 128,554.2844 | 128,128.2 | 127,085.5386 | 127,008.9 | 128,514 | 125,100.2 |
| | Mean | 130,615.4572 | 129,486 | 129,414.4588 | 128,315.4 | 129,495.4 | 125,263.2 |
| | Std | $1.19 \times 10^3$ | $1.02 \times 10^3$ | $9.84 \times 10^2$ | $2.16 \times 10^2$ | $6.93 \times 10^2$ | 85.3092 |
| | Mean time (s) | 54.74 | 55.85 | 48.51 | 48.35 | 75.3 | 47.88 |
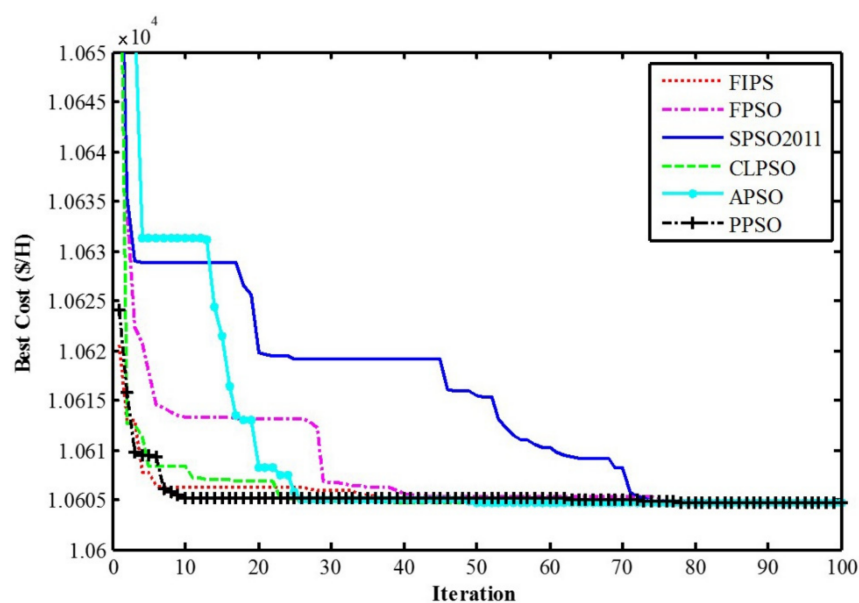


**Figure 3.** Convergence graphs of different PSO algorithms for the small-scale test system.

Furthermore, the cost function convergence graphs of the PSO algorithms of the multi-area power systems are shown in Figures 4 and 5, which show the superiority of the PPSO optimizer.



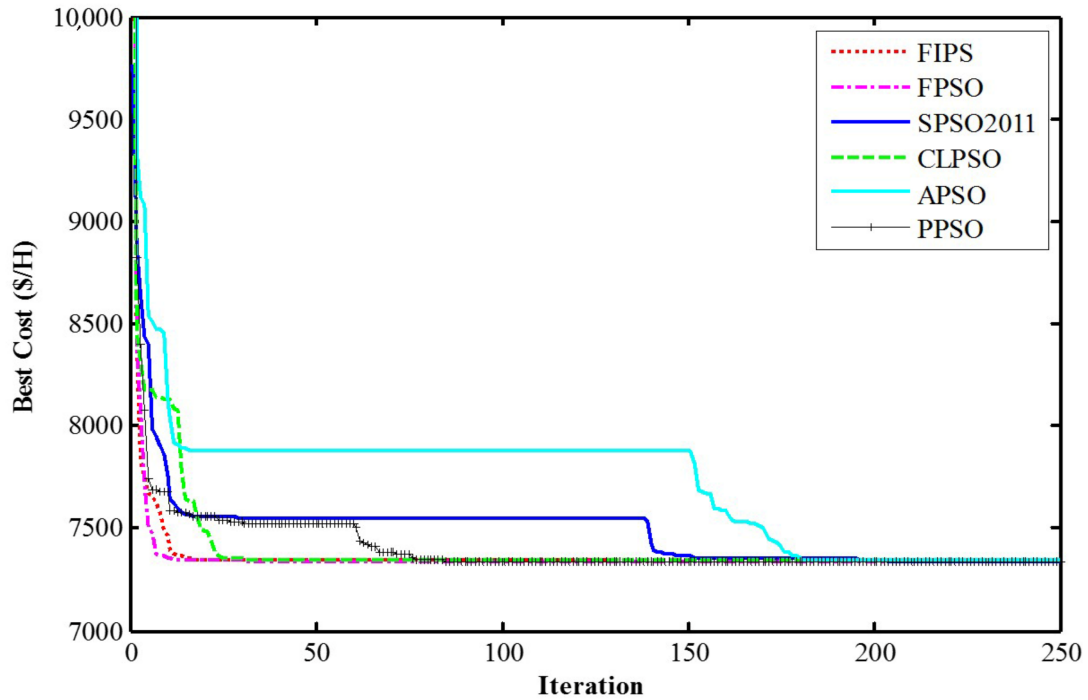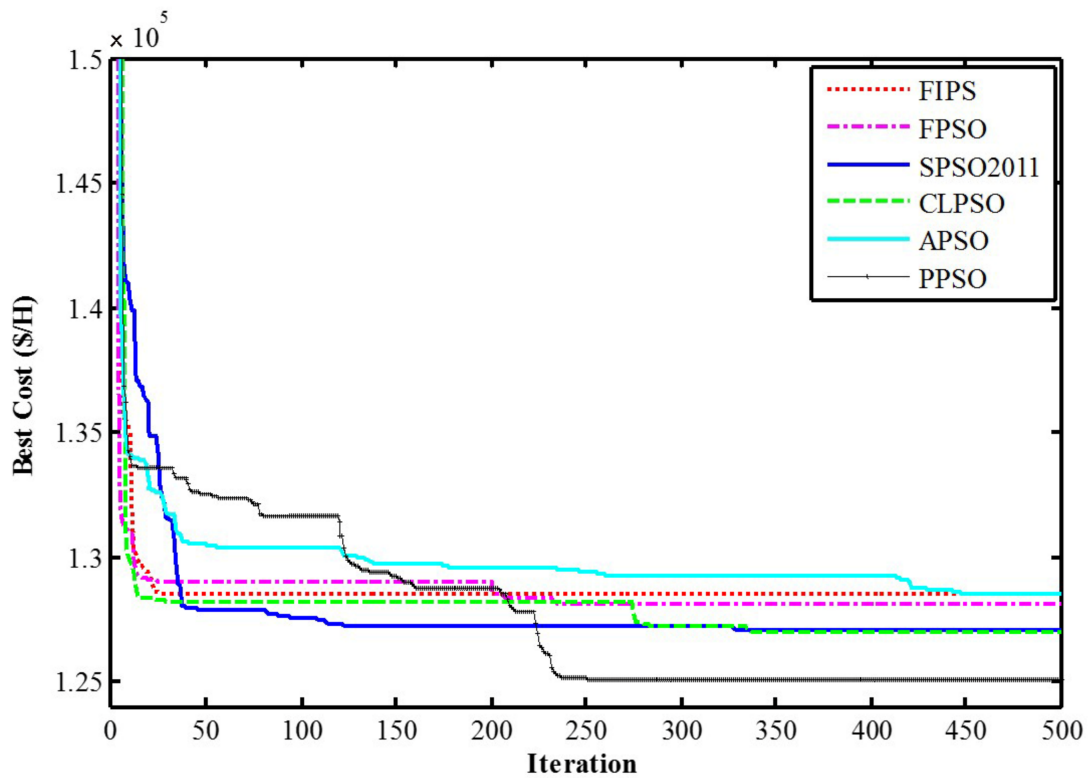**Figure 4.** Convergence graphs of different PSO algorithms for the medium-scale test system.



**Figure 5.** Convergence graphs of different PSO algorithms for the large-scale test system.

### 4.1.3. RCMAEED and RCMAED Problems

As mentioned before, the medium-scale four-area test power system, previously introduced, was selected for this part of the study. The fuel cost and pollutant emissions objective functions characteristics data and operating constraints of all generating units and tie-line minimum and maximum limits were extracted from [36]. The power demands are 30 MW in the 1st area, 50 MW in the 2nd area, 40 MW in the 3rd area, and 60 MW in the 4th area. The $S_{q,req}$ (SR requirement) for each area is 30% of the area power demand of that area, i.e., 9 MW, 15 MW, 12 MW, and 18 MW for areas 1 to 4, respectively. The maximum number of iterations and maximum population size were set to 500 and $N_{Pop}$ = 120, respectively, and $\phi$ was also set to 120 for the RCMAEED optimization problem. The global optimal results for the RCMAED and RCMAEED problems obtained using all the PSO optimizers are given in Tables 5 and 6, respectively. The tables show that the best solutions to the RCMAED and RCMAEED problems were obtained by the proposed PPSO optimizer; the optimizer was found to be superior to all other variants of PSO.

**Table 5.** Optimization results obtained by the PSO optimizers for the RCMAED problem for the four-area power system.

| Output (MW) | FIPS | FPSO | SPSO2011 | CLPSO | APSO | PPSO |
|---|---|---|---|---|---|---|
| $P_1$ | 8.5605 | 8.7146 | 8.1347 | 9.9192 | 8.468 | 11.1868 |
| $P_2$ | 9.9835 | 10 | 8.011 | 7.259 | 8.011 | 9.9596 |
| $P_3$ | 11.26 | 12.3534 | 13 | 8.7913 | 12.7035 | 6.6997 |
| $P_4$ | 0.2616 | 0.05 | 1.9639 | 4.8491 | 1.605 | 2.982 |
| $P_5$ | 18.807 | 22.1526 | 19.5629 | 23.6046 | 20.1371 | 22.8244 |
| $P_6$ | 11.261 | 9.4047 | 10.9592 | 9.2998 | 8.8157 | 8.8553 |
| $P_7$ | 6.1084 | 3.833 | 2.1895 | 3.9163 | 4.7532 | 3.9286 |
| $P_8$ | 15.2128 | 17.2551 | 17.925 | 16.3556 | 17.925 | 17.2481 |
| $P_9$ | 4.6622 | 6.0147 | 2.9329 | 6.1264 | 22.0733 | 5.8222 |
| $P_{10}$ | 10.5192 | 6.1858 | 8.5093 | 0.05 | 5.3173 | 0.1993 |
| $P_{11}$ | 20.4782 | 9.1548 | 23.2033 | 9.8982 | 7.4855 | 9.6888 |
| $P_{12}$ | 4.0058 | 17.2236 | 5.1026 | 22.3468 | 5.1026 | 22.8171 |
| $P_{13}$ | 11 | 8.1669 | 9.8282 | 9.1629 | 9.8282 | 8.0614 |
| $P_{14}$ | 20 | 19.7135 | 17.7366 | 19.9614 | 17.7366 | 19.8021 |
| $P_{15}$ | 26.8153 | 28.7234 | 30 | 28.1791 | 30 | 29.8714 |
| $P_{16}$ | 0.1384 | 1.2864 | 0.05 | 0.0869 | 0.05 | 0.0534 |
| $P_{17}$ | 0.1275 | 0.9452 | 0.5512 | 0.1 | 0.5512 | 0.486 |
| $P_{18}$ | 0.3016 | 0.2525 | 0.2146 | 0.2701 | 0.1433 | 0.204 |
| $P_{19}$ | 0.1 | 0.18 | 0.3539 | 0.3648 | 0.143 | 0.138 |
| $P_{20}$ | 0.1 | 1.4402 | 0.1105 | 1.4421 | 0.1105 | 1.4566 |
| $P_{21}$ | 1.1012 | 1.8441 | 1.1357 | 1.84 | 1.8756 | 1.8858 |
| $P_{22}$ | 0.1 | 0.1 | 0.2364 | 0.1034 | 0.2364 | 0.188 |
| $RC_{12}$ | 1.6842 | 2.2985 | 0.3671 | 0.6544 | 2.5336 | 1.5336 |
| $RC_{13}$ | 0.2249 | 0.1 | 0.1 | 0.8206 | 0.1 | 0.5945 |
| $RC_{14}$ | 1.8788 | 1.3163 | 2.1507 | 0.2931 | 1.05 | 0.1674 |
| $RC_{23}$ | 0.4049 | 0.2073 | 0.1 | 0.1 | 1.0058 | 0.1001 |
| $RC_{24}$ | 0.1645 | 2.4179 | 1.0183 | 1.6712 | 1.0183 | 2.1473 |
| $RC_{34}$ | 0.4582 | 0.1 | 0.602 | 0.2867 | 0.602 | 0.3759 |
| Reserve area 1 | 18.9344 | 17.882 | 17.8904 | 18.1814 | 18.2125 | 18.1719 |
| Reserve area 2 | 23.6108 | 22.3546 | 24.3634 | 21.8237 | 23.369 | 22.1436 |
| Reserve area 3 | 80.3346 | 81.4211 | 80.2519 | 81.5786 | 80.0213 | 81.4726 |
| Reserve area 4 | 33.0463 | 33.1098 | 33.3852 | 33.6097 | 33.3852 | 33.2117 |
| Best Cost ($) | 2187.418 | 2178.6024 | 2188.247 | 2171.0535 | 2193.541 | 2166.377 |
| Mean Cost ($) | 2700.367 | 2634.0676 | 2461.538 | 2494.3471 | 2510.7 | 2185.794 |
| Std | 363.4401 | 325.6323 | 204.1498 | 182.2067 | 250.0191 | 13.7298 |
| Time (s) | 69.34 | 66.06 | 54.48 | 52.27 | 77.31 | 51.93 |

**Table 6.** Optimization results obtained by PSO optimizers for the RCMAEED problem for the four-area power system.

| Output (MW) | FIPS | FPSO | SPSO2011 | CLPSO | APSO | PPSO |
|---|---|---|---|---|---|---|
| $P_1$ | 8.2773 | 10 | 8.2773 | 0.05 | 10.0006 | 10.0005 |
| $P_2$ | 5.444 | 5.3234 | 5.444 | 5.2116 | 5.3258 | 5.3259 |
| $P_3$ | 6.9757 | 7.0561 | 6.9757 | 12.3788 | 7.049 | 7.0491 |
| $P_4$ | 7.4634 | 11.998 | 7.4634 | 11.2161 | 11.9979 | 11.9978 |
| $P_5$ | 21.3822 | 9.9619 | 21.3822 | 16.8448 | 9.9143 | 12.2994 |
| $P_6$ | 7.3638 | 11.3019 | 7.3638 | 2.117 | 11.2907 | 11.3626 |
| $P_7$ | 7.6367 | 14.5624 | 12.0773 | 12.9769 | 14.5612 | 14.6209 |
| $P_8$ | 18 | 12.6441 | 14.0655 | 13.6205 | 12.7082 | 10.191 |
| $P_9$ | 17.3563 | 13.2916 | 17.3563 | 16.4181 | 13.2926 | 13.2921 |
| $P_{10}$ | 0.05 | 0.0891 | 0.05 | 0.05 | 0.0917 | 0.0919 |
| $P_{11}$ | 13.6655 | 13.0317 | 13.6655 | 3.4361 | 12.6414 | 12.618 |
| $P_{12}$ | 8.1572 | 14.2427 | 8.1572 | 19.1587 | 14.6307 | 14.6544 |
| $P_{13}$ | 9.2933 | 4.7521 | 9.2933 | 8.7209 | 4.753 | 4.7537 |
| $P_{14}$ | 12.6671 | 15.4968 | 11.2406 | 12.7486 | 15.4936 | 15.4934 |
| $P_{15}$ | 17.339 | 11.813 | 17.339 | 11.364 | 11.8142 | 11.8143 |
| $P_{16}$ | 20.0235 | 24.4354 | 20.0235 | 30 | 24.4352 | 24.435 |
| $P_{17}$ | −1.8289 | 1.19 | −1.8289 | 4.3668 | 1.1836 | 1.1836 |
| $P_{18}$ | −2.035 | −0.3652 | −2.035 | −1.7739 | −0.3653 | −0.3653 |
| $P_{19}$ | 1.7937 | 3.5526 | 1.0664 | −1.7123 | 3.555 | 3.555 |
| $P_{20}$ | 3.2182 | 0.1308 | 3.0699 | 0.6117 | 0.1288 | 0.1288 |
| $P_{21}$ | −2.1972 | −0.47 | −0.0632 | −0.925 | −0.4709 | −0.4713 |
| $P_{22}$ | 0.842 | 0.4207 | 0.842 | 0.8286 | 0.4199 | 0.4199 |
| $RC_{12}$ | −2.6122 | 0.4371 | −2.6122 | −1.1046 | 0.4376 | 0.4355 |
| $RC_{13}$ | 1.8735 | −3.5706 | 1.3435 | 0.4457 | −3.4213 | −3.396 |
| $RC_{14}$ | 3.3365 | −5.3328 | −10.8828 | −7.5176 | −5.4329 | −4.638 |
| $RC_{23}$ | −2.5379 | 0.2241 | −0.901 | 2.0858 | 0.2103 | 0.2071 |
| $RC_{24}$ | 0.6483 | −2.7136 | 0.6483 | −1.8365 | −2.0113 | −3.0807 |
| $RC_{34}$ | −0.5127 | −0.6214 | −0.5127 | −0.2932 | −0.7097 | −0.6741 |
| Reserve area 1 | 20.8396 | 14.6225 | 20.8396 | 20.1435 | 14.6267 | 14.6267 |
| Reserve area 2 | 20.6173 | 26.5297 | 20.1112 | 29.4408 | 26.5256 | 26.5261 |
| Reserve area 3 | 80.771 | 79.3449 | 80.771 | 80.9371 | 79.3436 | 79.3436 |
| Reserve area 4 | 31.6771 | 34.5027 | 33.1036 | 28.1665 | 34.504 | 34.5036 |
| Cost ($) | 2197.8688 | 2185.4666 | 2194.0611 | 2189.6647 | 2185.0785 | 2184.0477 |
| Emission (ton) | 3.6756 | 3.4257 | 3.5176 | 4.2518 | 3.4288 | 3.4097 |

### 4.1.4. Reliability-Oriented MAED

As mentioned earlier, reliability is one of the major issues in power system planning and operation. In this study, the cost of energy not supplied (CENS) is investigated as a reliability index in addition to optimizing the operational cost. Table 7 depicts the extracted results of the large-scale test system in the case of considering CENS. The results are different from the case without considering CENS. In this case, the value of ENS is 1.067 (MW); accordingly, the CENS is 7469 ($). Although the operation cost is increased in the case of considering reliability with 2.23%, it is worth mentioning that the ENS value for the case without considering reliability is 2.11 (MW); accordingly, the CENS and total operational cost are 14,770 $ and 139,870.2 $, respectively. In other words, the total operational cost decreased by 3.22%. As a result, solving the proposed problem from the perspective of reliability led to obtaining a solution with an appropriate level of reliability and smaller total operational cost.

**Table 7.** The obtained values for the proposed reliability-oriented MAED problem for the large-scale test system.

| Unit | Output (MW) | Unit | Output (MW) |
|---|---|---|---|
| $P_1$ | 114 | $P_{21}$ | 513.66 |
| $P_2$ | 114 | $P_{22}$ | 513.66 |
| $P_3$ | 120 | $P_{23}$ | 513.66 |
| $P_4$ | 180 | $P_{24}$ | 513.66 |
| $P_5$ | 97 | $P_{25}$ | 513.66 |
| $P_6$ | 140 | $P_{26}$ | 302.097 |
| $P_7$ | 300 | $P_{27}$ | 10 |
| $P_8$ | 266 | $P_{28}$ | 10 |
| $P_9$ | 266 | $P_{29}$ | 10 |
| $P_{10}$ | 270 | $P_{30}$ | 90 |
| $P_{11}$ | 126.2842 | $P_{31}$ | 190 |
| $P_{12}$ | 300 | $P_{32}$ | 188 |
| $P_{13}$ | 300 | $P_{33}$ | 140.55 |
| $P_{14}$ | 393.66 | $P_{34}$ | 152.1113 |
| $P_{15}$ | 482.666 | $P_{35}$ | 148.345 |
| $P_{16}$ | 490.1 | $P_{36}$ | 148.345 |
| $P_{17}$ | 481.76 | $P_{37}$ | 91.55 |
| $P_{18}$ | 484.55 | $P_{38}$ | 91.55 |
| $P_{19}$ | 550 | $P_{39}$ | 91.55 |
| $P_{20}$ | 523.9797 | $P_{40}$ | 267.6017 |
| T12 (MW) | | | −1500 |
| Operation Cost ($) | | | 127,893.5 |
| CENS ($) | | | 7469 |
| Total Cost | | | 135,362.5 |

*4.2. Discussion*

According to the results obtained in this paper, it can be concluded that the proposed algorithm can be a very simple, effective, and widely-used version of the well-known PSO algorithm. Based on the comparisons made between the proposed method and some available PSO algorithms, including adaptive PSO (APSO), comprehensive learning PSO (CLPSO), fully informed particle swarm (FIPS), Frankenstein's PSO (FPSO), and the improved standard PSO 2011 (SPSO2011) as well as several algorithms selected from recently-published papers, e.g., HNN [33], DSM [32], PSO-TVAC [32], PSO [9], HHS [12], NFP [37], CEP [36], PS [38], HSLSO [9], and DEC2 [7], it was concluded that the proposed method can be effectively applied to different problems in the field of energy and engineering optimization. Furthermore, considering the emission of units, reserve load, and system demand, the economic dispatching problem was analyzed practically and comprehensively.

**5. Conclusions**

Multi-area economic dispatch (MAED) is a very important issue in power systems, which affects the transmission of electrical energy. In this study, the cost associated with system reliability was added to the operational cost of the thermal unit in MAED for the first time. The objective function of the problem comprises three main terms: operational cost, the costs due to reliability, and emission factors. Regarding various types of technical limitations as well as the spinning reserve capacity, the paper proposed a new, improved version of particle swarm optimization (PSO), i.e., the phasor particle swarm optimization (PPSO) algorithm, to tackle complex optimization problems. The algorithm uses phasor theory in mathematics to define a new method for creating PSO control parameters and it was applied to optimal MAED problems in the context of different simulation tests. While in the first test the superiority of the PPSO algorithm was confirmed in terms of quality, reliability, and robustness in comparison to the existing algorithms of PSO, including adaptive PSO (APSO), comprehensive learning PSO (CLPSO), fully informed

particle swarm (FIPS), Frankenstein's PSO (FPSO), and the improved standard PSO 2011 (SPSO2011), the following tests focused on the impact of reliability considerations on the MAED and RCMAEED.

The obtained optimal results revealed that the proposed algorithm is strong and efficient for optimizing power dispatch in energy systems. In addition, it enjoys a special simplicity compared to its counterparts. Furthermore, the application of phasor theory in different types of improved PSO algorithms, including the proposed PPSO, can be further elaborated in different power system optimization problems for future studies.

**Author Contributions:** A.N., conceptualization; A.K., validation; Z.A.-M., supervision; I.F.D., writing—original draft; M.W.B.M., methodology; J.M.G., investigation. All authors have read and agreed to the published version of the manuscript.

**Institutional Review Board Statement:** Not applicable.

**Informed Consent Statement:** Not applicable.

**Data Availability Statement:** Data sharing not applicable. No new data were created or analyzed in this study.

## Abbreviations

**Indices:**

| | |
|---|---|
| $lp$ : | Load point index |
| $n$ : | Committed generation units $\epsilon\ [1,\ldots,\ N]$ |
| $k$ : | Input fuel types $\epsilon\ [1,\ldots,\ K]$ |
| $j$ : | Transmission lines $\epsilon\ [1,\ldots,\ M]$ |
| $q,\ w$ : | Area's index |
| $d$ : | Decision variable's index |
| $D$ : | The number of decision variables |
| $h$ : | The $h^{\text{th}}$ prohibited operating zones (POZ) |
| $H/H'$ | The $H/H'^{\text{th}}$ available/unavailable generation units |
| $M_q$ : | Set of all areas which are connected to $q$th area |

**Parameters:**

| | |
|---|---|
| $N_q$ : | The number of committed generating units in the $q$th area |
| $Std$ : | Standard deviation |
| $zn$ : | The number of POZs in the $n$th thermal unit power curve |
| $a_n,\ b_n,\ c_n,\ e_n,\ f_n$ : | The fuel cost coefficients of $n$th thermal unit |
| $a_{ik},\ b_{ik},\ c_{ik},\ e_{ik},\ f_{ik}$ : | The fuel cost coefficients of $n$th thermal unit for $k$th fuel type |
| $DR_n$ : | The down ramp rate-limit of $n$th thermal unit |
| $UR_n$ : | The up ramp rate-limits of $n$th thermal unit |
| $P_n^0$ : | The power output of $n$th thermal unit in the first stage |
| $P_{n,min}$ : | The minimum power output of $n$th thermal unit |
| $P_{n,max}$ : | The maximum power output of $n$th thermal unit |
| $P_{nk,min}$ : | The minimum power output of $n$th thermal unit for $k$th fuel type |
| $P_{nk}$ : | The maximum power output of $n$th thermal unit for $k$th fuel type |
| $P_{nh}^l$ : | The lower bound for prohibited zone k of $n$th thermal unit |
| $P_{nh}^u$ : | The upper bound for prohibited zone k of $n$th thermal unit |
| $P_{Load}$ : | System total load demand |
| $P_{Loadq}$ : | The power demand in $q$th area |
| $T_{qw,\ max}$ : | The maximum capacity of the tie-line between $q$th and $w$th areas |

| | |
|---|---|
| $\alpha_{nk}, \beta_{nk}, \gamma_{nk},:$ | The emission coefficients of $n$th thermal unit for $k$th fuel type |
| $S_{q, req}:$ | The spinning reserve requirement in the $q$th area |
| $\varphi:$ | User defined weighting factor for emission cost (in this study: 120) |
| $\lambda:$ | Penalty coefficient value |
| $N_{Pop}:$ | Number of initial population |
| $X_i:$ | The current position vector of $i$th particle |
| $V_i:$ | The current velocity vector of $i$th particle |
| $Iter_{max}:$ | Maximum number of iterations for PSO algorithm |
| $Pbest_i:$ | The best personal position vector of $i$th particle |
| $Gbest:$ | The global best position vector |
| $\theta:$ | The phase angle |
| $c_{ens}:$ | The cost of energy not supplied (7 \$/kWh) |
| $EPNS_{lp}:$ | Expected power not supplied at lp$^{\text{th}}$ load point |
| $TD_{lp}:$ | The time duration of lp$^{\text{th}}$ load point |
| $Probability_{lp}$ | The probability of availability and unavailability of generation |
| $X/Y$ | The set of available (unavailable) generation units |
| $FR_n$ | The failure rate of $n$th generator |
| $RR_n$ | The repair rate of $n$th generator |
| $MTTR_n$ | Mean time to repair $n$th generator |
| $MTTF_n$ | Mean time to failure of $n$th generator |
| $T_{Failure,n}$ | Failure time of $n$th generator |
| $T_{Repair,n}$ | Repair time of $n$th generator |
| $U_n$ | Unavailability (force outage rate) of $n$th generator |

**Functions and Variables:**

| | |
|---|---|
| $F_T$ | Objective function |
| $F_n(P_n):$ | The fuel cost function of $n$th thermal unit |
| $P_n:$ | The power output of $n$th thermal unit |
| $f_j:$ | Cost function associated with $j$th transmission line |
| $T_j:$ | Active power flow through $j$th transmission line |
| $T_{qw}:$ | The power flow from $q$th area to $w$th area |
| $E_n(P_n):$ | The emission function of $n$th thermal unit |
| $RC_{wq}:$ | The amount of reserve contributed between $q$th and $w$th areas |
| $S_n$ | The reserve provided by all thermal units in the $n$th area |

**Abbreviations:**

| | |
|---|---|
| APSO: | Adaptive PSO |
| CEP: | Classical evolutionary programming |
| CENS | Cost of energy not supplied |
| CLPSO: | Comprehensive learning PSO |
| DEC2: | Chaotic DE/2 algorithm |
| DSM: | Direct search method |
| EENS: | Expected energy not supplied |
| ELD: | Economic load dispatch |
| EP: | Evolutionary programming |
| FIPS: | Fully informed particle swarm |
| FPSO: | Frankenstein's PSO |
| HNN: | Hopfield neural network |
| HS: | Harmony search |
| HSLSO: | Hybridizing sum-local search optimizer |
| LOLP: | Loss of Load Probability |
| MAED: | Multi-area economic dispatch |
| NFP: | Network flow programming |
| POZ: | Prohibited operating zones |
| PPSO: | Phasor particle swarm optimization |
| PS: | Pattern search |
| PSO: | Particle swarm optimization |
| PSO-cf: | Modified PSO by constriction factor |
| PSO-TVAC: | Self-organizing hierarchical particle swarm optimizer with time-varying acceleration coefficients |

| PSO-ω: | Modified PSO by the inertia weight |
|---|---|
| RCMAED: | Reserve constrained multi-area economic dispatch |
| RCMAEED: | Reserve constrained multi-area environmental/economic dispatch |
| SPSO2011: | The improved standard PSO 2011 |
| SR: | Spinning reserve |
| VPL: | Valve-point loading |

## References

1.  Naderipour, A.; Abdul-Malek, Z.; Nowdeh, S.A.; Ramachandaramurthy, V.K.; Kalam, A.; Guerrero, J.M. Optimal allocation for combined heat and power system with respect to maximum allowable capacity for reduced losses and improved voltage profile and reliability of microgrids considering loading condition. *Energy* **2020**, *196*, 117124. [CrossRef]
2.  Fu, C.; Zhang, S.; Chao, K.-H. Energy management of a power system for economic load dispatch using the artificial intelligent algorithm. *Electronics* **2020**, *9*, 108. [CrossRef]
3.  Fu, B.; Ouyang, C.; Li, C.; Wang, J.; Gul, E. An improved mixed integer linear programming approach based on symmetry diminishing for unit commitment of hybrid power system. *Energies* **2019**, *12*, 833. [CrossRef]
4.  Abido, M.A. Multiobjective evolutionary algorithms for electric power dispatch problem. *IEEE Trans. Evol. Comput.* **2006**, *10*, 315–329. [CrossRef]
5.  Ren, Y.; Fei, S. The auxiliary problem principle with self-adaptive penalty parameter for multi-area economic dispatch problem. *Algorithms* **2015**, *8*, 144–156. [CrossRef]
6.  Nowdeh, S.A.; Nasri, S.; Saftjani, P.B.; Naderipour, A.; Abdul-Malek, Z.; Kamyab, H.; Nowdeh, A.J. Multi-Criteria Optimal Design of Hybrid Clean Energy System with Battery Storage Considering Off- and On-Grid Application. *J. Clean. Prod.* **2020**. [CrossRef]
7.  Abdollahi, E.; Wang, H.; Lahdelma, R. An optimization method for multi-area combined heat and power production with power transmission network. *Appl. Energy* **2016**, *168*, 248–256. [CrossRef]
8.  Sharma, M.; Pandit, M.; Srivastava, L. Reserve constrained multi-area economic dispatch employing differential evolution with time-varying mutation. *Int. J. Electr. Power Energy Syst.* **2011**, *33*, 753–766. [CrossRef]
9.  Yu, J.; Kim, C.-H.; Wadood, A.; Khurshiad, T.; Rhee, S.-B. A novel multi-population based chaotic JAYA algorithm with application in solving economic load dispatch problems. *Energies* **2018**, *11*, 1946. [CrossRef]
10.  Ghasemi, M.; Aghaei, J.; Akbari, E.; Ghavidel, S.; Li, L. A differential evolution particle swarm optimizer for various types of multi-area economic dispatch problems. *Energy* **2016**, *107*, 182–195. [CrossRef]
11.  Jadoun, V.K.; Gupta, N.; Niazi, K.R.; Swarnkar, A. Modulated particle swarm optimization for economic emission dispatch. *Int. J. Electr. Power Energy Syst.* **2015**, *73*, 80–88. [CrossRef]
12.  Ghasemi, A. A fuzzified multi objective interactive honey bee mating optimization for environmental/economic power dispatch with valve point effect. *Int. J. Electr. Power Energy Syst.* **2013**, *49*, 308–321. [CrossRef]
13.  Dubey, H.M.; Pandit, M.; Tyagi, N.; Panigrahi, B.K. Wind integrated multi area economic dispatch using backtracking search algorithm. In Proceedings of the 2016 IEEE 6th International Conference on Power Systems (ICPS), New Delhi, India, 4–6 March 2016; pp. 1–6.
14.  Mokarram, M.J.; Niknam, T.; Aghaei, J.; Shafie-khah, M.; Catalao, J.P.S. Hybrid optimization algorithm to solve the nonconvex multiarea economic dispatch problem. *IEEE Syst. J.* **2019**, *13*, 3400–3409. [CrossRef]
15.  Vijayaraj, S.; Santhi, R.K. Multi-Area economic dispatch using flower pollination algorithm. In Proceedings of the 2016 International Conference on Electrical, Electronics, and Optimization Techniques (ICEEOT), Chennai, India, 3–5 March 2016; pp. 4355–4360.
16.  Azizipanah-Abarghooee, R.; Dehghanian, P.; Terzija, V. Practical multi-area bi-objective environmental economic dispatch equipped with a hybrid gradient search method and improved Jaya algorithm. *IET Gener. Transm. Distrib.* **2016**, *10*, 3580–3596. [CrossRef]
17.  Lin, J.; Wang, Z.-J. Multi-Area economic dispatch using an improved stochastic fractal search algorithm. *Energy* **2019**, *166*, 47–58. [CrossRef]
18.  Ghasemi, M.; Davoudkhani, I.F.; Akbari, E.; Rahimnejad, A.; Ghavidel, S.; Li, L. A novel and effective optimization algorithm for global optimization and its engineering applications: Turbulent Flow of Water-based Optimization (TFWO). *Eng. Appl. Artif. Intell.* **2020**, *92*, 103666. [CrossRef]
19.  Nguyen, K.P.; Dinh, N.D.; Fujita, G. Multi-Area economic dispatch using Hybrid Cuckoo search algorithm. In Proceedings of the 2015 50th International Universities Power Engineering Conference (UPEC), Stoke on Trent, UK, 1–4 September 2015; pp. 1–6.
20.  Basu, M. Artificial bee colony optimization for multi-area economic dispatch. *Int. J. Electr. Power Energy Syst.* **2013**, *49*, 181–187. [CrossRef]
21.  Chen, C.-L.; Chen, Z.-Y.; Lee, T.-Y. Multi-Area economic generation and reserve dispatch considering large-scale integration of wind power. *Int. J. Electr. Power Energy Syst.* **2014**, *55*, 171–178. [CrossRef]
22.  Secui, D.C. The chaotic global best artificial bee colony algorithm for the multi-area economic/emission dispatch. *Energy* **2015**, *93*, 2518–2545. [CrossRef]

23. Ghasemi, M.; Ghavidel, S.; Aghaei, J.; Akbari, E.; Li, L. CFA optimizer: A new and powerful algorithm inspired by Franklin's and Coulomb's laws theory for solving the economic load dispatch problems. *Int. Trans. Electr. Energy Syst.* **2018**, *28*, e2536. [CrossRef]

24. Shi, Y.; Eberhart, R. A modified particle swarm optimizer. In Proceedings of the 1998 IEEE International Conference on Evolutionary Computation Proceedings, IEEE World Congress on Computational Intelligence (Cat. No. 98TH8360), Anchorage, AK, USA, 4–9 May 1998; pp. 69–73.

25. Laganà, D.; Mastroianni, C.; Meo, M.; Renga, D. Reducing the operational cost of cloud data centers through renewable energy. *Algorithms* **2018**, *11*, 145. [CrossRef]

26. Chaiyabut, N.; Damrongkulkumjorn, P. Optimal spinning reserve for wind power uncertainty by unit commitment with EENS constraint. In Proceedings of the ISGT, Washington, DC, USA, 19–22 February 2014; pp. 1–5.

27. Khokhar, S.; Zin, A.A.M.; Mokhtar, A.S.; Bhayo, M.A.; Naderipour, A. Automatic classification of single and hybrid power quality disturbances using Wavelet Transform and Modular Probabilistic Neural Network. In Proceedings of the 2015 IEEE Conference on Energy Conversion, CENCON 2015, Johor Bahru, Malaysia, 19–20 October 2015; pp. 457–462.

28. Ajmal, A.M.; Ramachandaramurthy, V.K.; Naderipour, A.; Ekanayake, J.B. Comparative analysis of two-step GA-based PV array reconfiguration technique and other reconfiguration techniques. *Energy Convers. Manag.* **2021**, *230*, 113806. [CrossRef]

29. Naderipour, A.; Abdul-Malek, Z.; Nowdeh, S.A.; Kamyab, H.; Ramtin, A.R.; Shahrokhi, S.; Klemeš, J.J. Comparative evaluation of hybrid photovoltaic, wind, tidal and fuel cell clean system design for different regions with remote application considering cost. *J. Clean. Prod.* **2020**. [CrossRef]

30. Naderipour, A.; Abdul-Malek, Z.; Nowdeh, S.A.; Gandoman, F.H.; Moghaddam, M.J.H. A multi-objective optimization problem for optimal site selection of wind turbines for reduce losses and improve voltage profile of distribution grids. *Energies* **2019**, *12*, 2621. [CrossRef]

31. Naderipour, A.; Abdul-Malek, Z.; Vahid, M.Z.; Seifabad, Z.M.; Hajivand, M.; Arabi-Nowdeh, S. Optimal, reliable and cost-effective framework of photovoltaic-wind-battery energy system design considering outage concept using grey wolf optimizer algorithm—Case study for iran. *IEEE Access* **2019**, *7*, 182611–182623. [CrossRef]

32. Lasemi, M.A.; Assili, M.; Baghayipour, M. Modification of multi-area economic dispatch with multiple fuel options, considering the fuelling limitations. *IET Gener. Transm. Distrib.* **2014**, *8*, 1098–1106. [CrossRef]

33. Roy, P.K.; Hazra, S. Economic emission dispatch for wind–fossil-fuel-based power system using chemical reaction optimisation. *Int. Trans. Electr. Energy Syst.* **2015**, *25*, 3248–3274. [CrossRef]

34. Niknam, T. A new fuzzy adaptive hybrid particle swarm optimization algorithm for non-linear, non-smooth and non-convex economic dispatch problem. *Appl. Energy* **2010**, *87*, 327–339. [CrossRef]

35. Ganjefar, S.; Tofighi, M. Dynamic eNconomic dispatch solution using an improved genetic algorithm with non-stationary penalty functions. *Eur. Trans. Electr. Power* **2011**, *21*, 1480–1492. [CrossRef]

36. Wang, L.; Singh, C. Reserve-Constrained multiarea environmental/economic dispatch based on particle swarm optimization with local search. *Eng. Appl. Artif. Intell.* **2009**, *22*, 298–307. [CrossRef]

37. Jensi, R.; Jiji, G.W. An enhanced particle swarm optimization with levy flight for global optimization. *Appl. Soft Comput.* **2016**, *43*, 248–261. [CrossRef]

38. Clerc, M.; Kennedy, J. The particle swarm-explosion, stability, and convergence in a multidimensional complex space. *IEEE Trans. Evol. Comput.* **2002**, *6*, 58–73. [CrossRef]

39. Ratnaweera, A.; Halgamuge, S.K.; Watson, H.C. Self-Organizing hierarchical particle swarm optimizer with time-varying acceleration coefficients. *IEEE Trans. Evol. Comput.* **2004**, *8*, 240–255. [CrossRef]

40. Ghasemi, M.; Akbari, E.; Rahimnejad, A.; Razavi, S.E.; Ghavidel, S.; Li, L. Phasor particle swarm optimization: A simple and efficient variant of PSO. *Soft Comput.* **2019**, *23*, 9701–9718. [CrossRef]

41. Zhan, Z.-H.; Zhang, J.; Li, Y.; Chung, H.S.-H. Adaptive particle swarm optimization. *IEEE Trans. Syst. Man Cybern. Part* **2009**, *39*, 1362–1381. [CrossRef] [PubMed]

42. Liang, J.J.; Qin, A.K.; Suganthan, P.N.; Baskar, S. Comprehensive learning particle swarm optimizer for global optimization of multimodal functions. *IEEE Trans. Evol. Comput.* **2006**, *10*, 281–295. [CrossRef]

43. Zambrano-Bigiarini, M.; Clerc, M.; Rojas, R. Standard particle swarm optimisation 2011 at cec-2013: A baseline for future pso improvements. In Proceedings of the 2013 IEEE Congress on Evolutionary Computation, Cancun, Mexico, 20–23 June 2013; pp. 2337–2344.

44. Mendes, R.; Kennedy, J.; Neves, J. The fully informed particle swarm: Simpler, maybe better. *IEEE Trans. Evol. Comput.* **2004**, *8*, 204–210. [CrossRef]

45. De Oca, M.A.M.; Stutzle, T.; Birattari, M.; Dorigo, M. Frankenstein's PSO: A composite particle swarm optimization algorithm. *IEEE Trans. Evol. Comput.* **2009**, *13*, 1120–1132. [CrossRef]

46. Yalcinoz, T.; Short, M.J. Neural networks approach for solving economic dispatch problem with transmission capacity constraints. *IEEE Trans. Power Syst.* **1998**, *13*, 307–313. [CrossRef]

47. Chen, C.-L.; Chen, N. Direct search method for solving economic dispatch problem considering transmission capacity constraints. *IEEE Trans. Power Syst.* **2001**, *16*, 764–769. [CrossRef]

48. Fesanghary, M.; Ardehali, M.M. A novel meta-heuristic optimization methodology for solving various types of economic dispatch problem. *Energy* **2009**, *34*, 757–766. [CrossRef]

49. Pandit, M.; Srivastava, L.; Pal, K. Static/Dynamic optimal dispatch of energy and reserve using recurrent differential evolution. *IET Gener. Transm. Distrib.* **2013**, *7*, 1401–1414. [CrossRef]
50. Soroudi, A.; Rabiee, A. Optimal multi-area generation schedule considering renewable resources mix: A real-time approach. *IET Gener. Transm. Distrib.* **2013**, *7*, 1011–1026. [CrossRef]
51. Jayabarathi, V.; Ramachandran, T.G.S. Evolutionary programming-based multiarea economic dispatch with tie line constraints. *Electr. Mach. Power Syst.* **2000**, *28*, 1165–1176. [CrossRef]
52. Zhu, J.; Momoh, J.A. Multi-Area power systems economic dispatch using nonlinear convex network flow programming. *Electr. Power Syst. Res.* **2001**, *59*, 13–20. [CrossRef]
53. Al-Sumait, J.S.; Sykulski, J.K.; Al-Othman, A.K. Solution of different types of economic load dispatch problems using a pattern search method. *Electr. Power Compon. Syst.* **2008**, *36*, 250–265. [CrossRef]